Part III

Carbon Deposition Boundaries in the CHO System at Several Pressures

A. D. TEVEBAUGH[1] and E. J. CAIRNS, General Electric Research Laboratory, Schenectady, N. Y.

The carbon-deposition boundaries for the carbon-hydrogen-oxygen system have been computed to a high degree of precision for the temperature range 298° to 1300° K. at 1, 2.5, 5, 10, and 20 atmospheres total pressure. The location of the carbon-deposition boundary is determined by the temperature, pressure, and O/H ratio. The utility of the triangular coordinate representation of the carbon-deposition boundaries has been shown by means of an example. The secant method for the solution of simultaneous nonlinear equations was used.

ONLY recently has the thermodynamics of the CHO system become of interest over the entire composition range for various temperatures and pressures. Classical processes such as coal gasification, hydrogen production, and chemical synthesis have usually been concerned with the operating conditions of elevated temperatures and pressures. Low pressures and high temperatures have been of particular interest in combustion processes and magnetohydrodynamics. Newer technologies such as low-temperature, hydrocarbon-fuel cells (*1, 6, 7, 9*), low-temperature, water-gas shift processes (*4*), and purification of hydrogen from steam-reformed hydrocarbons (*11*) require a knowledge of the thermodynamics of the CHO system at low temperatures and low pressures. Although in the latter cases, where temperatures and pressures are low, the reactions occur at significant rates because highly active catalysts are generally used (*1, 8*). Under these conditions, carbonaceous deposits sometimes occur, and their presence is detrimental to catalyst effectiveness. A knowledge of the conditions under which carbon deposits can form is, therefore, important.

The CHO gas-phase composition in equilibrium with carbon, and the carbon-deposition boundaries at 1 atm. have previously been published (*2*). The present work is concerned with the carbon-deposition boundaries as a function of both temperature and pressure. The shift of the carbon-deposition boundaries with pressure is interpreted and discussed.

[1] Present address: Argonne National Laboratory, Chemical Engineering Division, 9700 Cass Ave., Argonne, Ill.

The carbon-deposition boundaries are presented on triangular coordinates; the utility of this method for presenting these data has been discussed (*2*). The triangular-coordinate presentation makes clear the application of the results to systems consisting of any CHO compound or mixture of compounds containing one or more of the elements hydrogen, carbon, and oxygen in any proportions. A specific application of this diagram is discussed.

THERMODYNAMIC METHODS

The C:H:O atom ratios in the gas phase in equilibrium with graphitic carbon (the carbon-deposition boundaries) were calculated by use of a high-speed digital computer, using methods similar to that previously reported (*2*), with a modification of the convergence procedure to that of the secant method (*5*). The thermodynamic-equilibrium constant data were obtained from APIRP No. 44 (*10*). These data set the maximum accuracy of the results at five significant figures at the low and high temperatures and four significant figures in the mid-range of temperature (900° K.).

The computer-input data were equilibrium constants for each temperature, O/H atom ratios (*2*), and total pressure. The values of C, H, and O for the gas phase in equilibrium with carbon (graphite) were computed such that C + H + O = 1 and were printed out in tabular form as a function of temperature, pressure, and O/H atom ratio. In addition, the C/H ratios for the gas phase in equilibrium with graphitic carbon were printed out as a function of the same variables. For these calculations, the six species H_2, H_2O,

C, CH_4, CO, and CO_2 were assumed to be the only species present in significant amounts at equilibrium. The validity of this assumption is supported by data and by the use of computational methods for trace species (C_2H_6, C_2H_4, C_2H_2, etc.) given in a previous publication (2).

RESULTS AND DISCUSSION

The most concise manner of summarizing the carbon-deposition boundary location is the listing of the C/H atom ratios of the gas phase as a function of the O/H atom ratio (gas phase) and temperature, for each pressure. These results are obtainable from ADI.

Figure 1 is a graphical presentation of the carbon-deposition boundaries computed from the results tabulated with ADI. The data for the graph at 1 atm. appear in a previous paper (2). The carbon-deposition boundary for a given temperature and pressure divides the triangular C-H-O diagram into two regions (Figure 1). The region above the carbon-deposition boundary (nearest the carbon apex) represents those over-all gas-phase CHO compositions which will deposit solid carbon (graphite) as they approach thermodynamic equilibrium. Gas-phase compositions which lie below the carbon-deposition boundary will not deposit solid carbon at thermodynamic equilibrium. The generality of the triangular coordinate presentation becomes clear when it is recognized that C:H:O ratios of the system completely determine whether or not carbon will form from a given reactant composition, temperature, and pressure.

The dashed lines for 950° and 1000° K. were obtained from the interpolation of large-scale cross-plots of the data calculated by the computer for the other temperatures. The intercepts on the C—H and C—O axes for 850°, 950°, 1000°, and 1050° K. were calculated from the following expressions:

C—O Axis

$$2\,CO \rightleftarrows CO_2 + C \tag{1}$$

$$K_{eq} = \frac{P_{CO_2}}{P^2_{CO}} \tag{2}$$

$$P_{CO_2} + P_{CO} = P_T \tag{3}$$

$$P_{CO} = \frac{-1 \pm (1 + 4\,P_T\,K_{eq})^{1/2}}{2\,K_{eq}} \tag{4}$$

C—H Axis

$$C + 2\,H_2 \rightleftarrows CH_4 \tag{5}$$

$$K^1_{eq} = \frac{P_{CH_4}}{P^2_{H_2}} \tag{6}$$

$$P_{CH_4} + P_{H_2} = P_T \tag{7}$$

$$P_{H_2} = \frac{-1 \pm (1 + 4\,P_T\,K^1_{eq})^{1/2}}{2\,K^1_{eq}} \tag{8}$$

The equilibrium constants were obtained from APIRP (*10*) and from large-scale plots of those values against 1/T. Table I summarizes the results of the intercept calculations for the C—H and C—O axes. The intercept data for 1 atm. pressure are given in a previous publication (2).

The heavy dashed lines for 298° K. at 1, 2.5, 5, 10, and 20 atm. (Figure 1) and for 400° K. at 5, 10, and 20 atm. (Figure 1) indicate that the calculations were performed as if all the water present at equilibrium were in the gas phase. Subsequent calculations using the computer data showed that liquid water would be present at equilibrium for a portion of the dashed boundaries. The heavy dashed lines at 298° and 400° K. are, therefore, most useful for interpolation purposes and do not represent a physically realistic equilibrium situation.

For the previous calculations of the gas-phase compositions at 1 atm. (2) (Figure 1), it is clear that the major species present at the higher temperatures are CO and H_2; therefore, the carbon-deposition boundaries for the higher temperatures are essentially straight lines joining the points representing CO and H_2 on the triangular diagram. At the lower temperatures, CH_4, H_2O, and CO_2 are most stable, and the carbon-deposition boundaries join CH_4 and CO_2, bowing strongly toward H_2O.

For those temperatures where thermal decomposition of methane to form hydrogen and carbon (Equation 5) results in comparable amounts of hydrogen and methane being present (at approximately 800° to 1000° K.), pressure has a noticeable effect in suppressing the decomposition reaction through the law of mass action. Thus, the carbon-deposition boundary intercepts on the C—H axis move toward CH_4 with increasing pressure. For the same reasons, the carbon-deposition boundary intercepts on the C—O axis move toward CO_2 with increasing pressure.

A quantitative expression of the pressure effects on the position of the C—O axis and C—H axis intercepts is obtained by the differentiation of the equilibrium constant for Equations 1 and 5 in terms of mole fractions with respect to pressure. The resultant expressions (equal to zero) are solved for $\left(\frac{\partial X_{CO}}{\partial \ln P}\right)_T$ and $\left(\frac{\partial X_{H_2}}{\partial \ln P}\right)_T$:

$$\left(\frac{\partial X_{CO}}{\partial \ln P}\right)_T = \frac{X_{CO}\,(X_{CO} - 1)}{(2 - X_{CO})} \tag{9}$$

$$\left(\frac{\partial X_{H_2}}{\partial \ln P}\right)_T = \frac{X_{H_2}\,(X_{H_2} - 1)}{(2 - X_{H_2})} \tag{10}$$

The composition at which the maximum pressure effect occurs is found by differentiation of Equations 9 and 10

Table I. Carbon Deposition Boundary Intercepts on the C—H and C—O Axes

T, ° K.	C—H Axis, Atom %C	C—O Axis, Atom %O
	P = 2.5 atm.	
850	13.68	65.15
950	8.96	61.62
1000	6.76	58.83
1050	4.89	55.89
	P = 5 atm.	
850	15.47	65.59
950	11.61	62.96
1000	9.49	60.71
1050	7.45	58.00
	P = 10 atm.	
850	16.79	65.90
950	13.87	63.99
1000	12.08	62.25
1050	10.18	59.98
	P = 20 atm.	
850	17.73	66.12
950	15.61	64.74
1000	14.24	63.45
1050	12.68	61.67

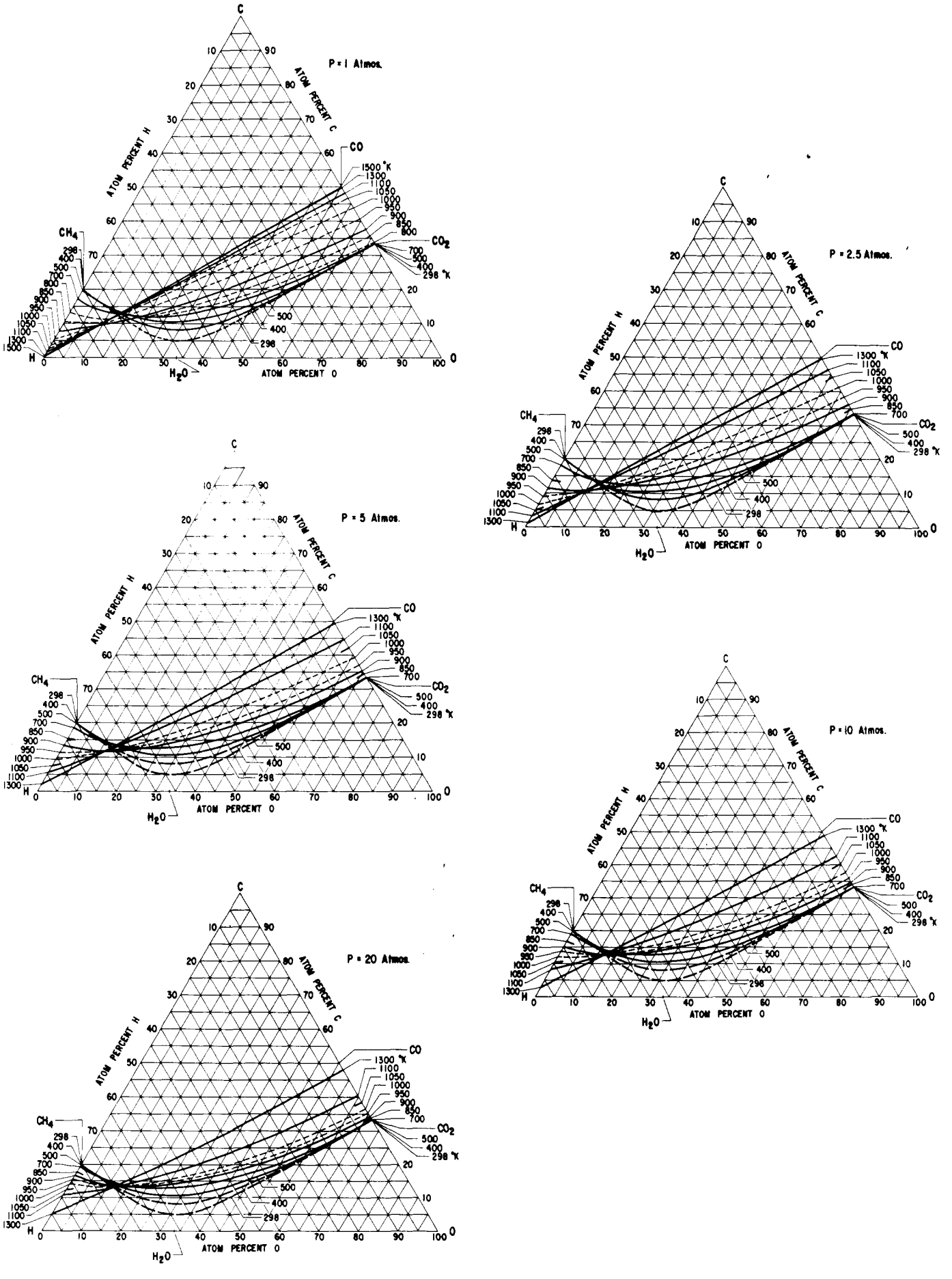

Figure 1. Carbon deposition boundaries for the CHO system at several pressures

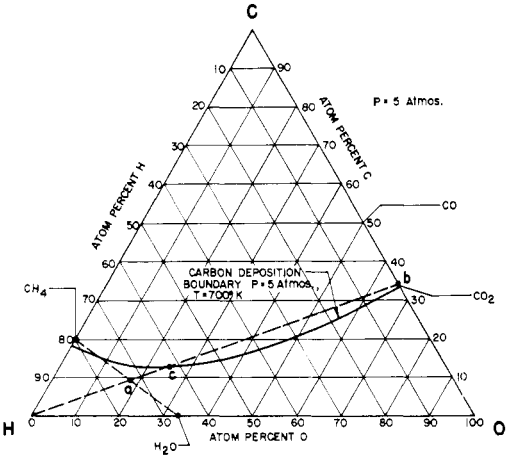

Figure 2. Gas phase composition change as hydrogen is removed from a steam reformer product stream

with respect to X_{CO} and X_{H_2}, respectively, setting the resultant expressions equal to zero and solving for X_{CO} and X_{H_2}, respectively. The maximum pressure effect occurs at $X_{CO} = 0.586$ (atom % C = 41.4) and $X_{H_2} = 0.586$ (atom % H = 87.2). The temperatures at which these maxima occur are a function of pressure, as can be seen by inspection of Figure 1.

The effect of having ignored trace species (C_2H_6, C_2H_4, C_2H_2, etc.) in the computer calculations was evaluated by methods similar to those described earlier (2). The carbon-deposition boundary positions at high O/H ratios (gas phase) were affected by less than 1 unit in the 8th significant figure by ignoring trace species. At low O/H ratios (< 0.1), the influence of trace species varied with temperature as follows: at low temperatures the C/H ratios were affected by less than 1 unit in the 8th significant figure, at 900° K., by 2 units in the 5th significant figure, and at 1300° K., 8 units in the 6th significant figure. The tabulated C/H values are too low by the above amounts.

The utility of the carbon-deposition boundaries and their triangular representation is best illustrated by an example. Consider the process of abstracting pure hydrogen from the product stream of a steam reformer by use of a silver-palladium diffuser membrane. The steam to methane ratio of the reformer feed is to be varied, and the amount of hydrogen which can be abstracted before carbon (graphite) will deposit on the diffuser membrane at thermodynamic equilibrium is to be calculated. The diffuser is to operate at 5 atm. pressure and 700° K. The compositions (expressed in atom %) of all mixtures of CH_4 and H_2O lie along a straight line joining the CH_4 point on the C—H axis and the H_2O point on the H—O axis of Figure 2. For a ratio of 2 moles of H_2O per mole of CH_4, the over-all atom per cents of the H_2O-CH_4 mixture are: %C = 9.09, %O = 18.18, %H = 72.73. This point (point *a*) is located on the H_2O-CH_4 line and also represents the over-all composition of the product stream from the steam reformer. As hydrogen is abstracted by the Ag-Pd diffuser, the over-all atom per cent composition of the residual gas in the diffuser varies along a straight line (line *H-a-b*) from the *H* apex of Figure 2 through the feed composition point (point *a*) on the CH_4-H_2O line to the C—O axis (intercept is point *b*). As hydrogen is abstracted, the residual gas composition moves from the feed composition point (point *a*) toward the C—O axis (point *b*). When the gas-phase composition reaches point *c* (Figure 2), carbon will deposit and the gas-phase composition will follow the carbon-deposition boundary as additional hydrogen is removed from the system. The line *H-a-b* will intersect the 700° K. carbon deposition boundary of Figure 2 at point *c* where %C = 12.7, %H = 62.1, %O = 25.2. A lever-rule calculation shows that 1.54 moles of H_2 can be abstracted per mole of feed CH_4 before carbon will deposit on the diffuser membrane at equilibrium.

An identical analysis can verify that a H_2O-to-CH_4 ratio of 3.5 in the reformer feed will result in a mixture from which hydrogen can be abstracted without encountering a carbon-deposition boundary at any temperature above 400° K. Related examples are given by Cairns, Tevebaugh, and Holm (3).

CONCLUSIONS

The carbon-deposition boundaries for the CHO system at 1, 2.5, 5, 10, and 20 atm. have been computed over the temperature range 298° to 1300° K. to a high degree of precision.

The utility of the triangular coordinate representation of the carbon-deposition boundaries has been shown by means of an example.

ACKNOWLEDGMENT

We are grateful to J.T. Godfrey and C.A. Tsonis for their help in programming and performing the computer calculations; also to Joyce E. Tevebaugh and Ann M. Coppola for their help with supplemental calculations and the plotting of data. We are indebted to E.A. Oster for making funds available for this work and to H.A. Liebhafsky for his encouragement in initiating these studies. This work is a part of the program under contract **DA-44-009-AMC-479(T)** and **DA-44-009-ENG-4909**, ARPA Order **No. 247** with the U. S. Army Engineer Research & Development Laboratories, Ft. Belvoir, Va., to develop a technology which will facilitate the design and fabrication of practical military fuel cell power plants for operation on ambient air and hydrocarbon fuels.

LITERATURE CITED

(1) Cairns, E.J., MacDonald, D.I., *Electrochem. Technol.* **2**, 65 (1964).
(2) Cairns, E.J., Tevebaugh, A.D., J. CHEM. ENG. DATA **9**, 453 (1964).
(3) Cairns, E.J., Tevebaugh, A.D., Holm, G.J., *J. Electrochem. Soc.* **110**, 1025 (1963).
(4) *Chem. Eng. News* **41**, 46 (Feb. 11, 1963).
(5) Godfrey, J.T., General Electric Advanced Technology Laboratories Rept. No. **63 GL 114**, 1963.
(6) Grubb, W.T., Michalske, C.J., *Nature* **201**, 287 (1964).
(7) Jasinski, R.J., Huff, J., Tomter, S., Swette, L., *Ber. Bunsenges. Physik. Chem.* **68**, 400 (1964).
(8) McKee, D.W., *J. Phys. Chem.* **67**, 841 (1963).
(9) Oswin, H.G., Hartner, A.J., Malaspina, F., *Nature* **200**, 256 (1963).
(10) Rossini, F.D., Pitzer, K.S., Arnett, R.L., Brown, R.M., Pimentel, G.C., American Petroleum Institute Research Project No. 44, Carnegie Press, Pittsburgh, Pa., 1953.
(11) Tevebaugh, A.D., Cairns, E.J., Saturated Hydrocarbon Fuel Cell Program (ARPA) Final Technical Summary Rept., Dec. 1, 1961-Dec. 31, 1962, Section II, Contract No. **DA-44-009-Eng-4853**, ARPA Order **No. 247-61.**

RECEIVED for review March 8, 1965. Accepted August 4, 1965. Tables of data supplementary to this article have been deposited as Document No. 8526 with the ADI Auxiliary Publications Project, Photoduplication Service, Library of Congress, Washington 25, D. C. A copy may be secured by citing the document number and by remitting $1.25 for photoprints, or $1.25 for 35 mm. microfilm. Advance payment is required. Make checks or money orders payable to: Chief, Photod[illegible] Service, Library of Congress.